PHYSICAL REVIEW B **78**, 140401(R) (2008)

Magnetoelectric control of spin-chiral ferroelectric domains in a triangular lattice antiferromagnet

Kenta Kimura,[1] Hiroyuki Nakamura,[1] Kenya Ohgushi,[2] and Tsuyoshi Kimura[1]
[1]*Division of Materials Physics, Graduate School of Engineering Science, Osaka University, Toyonaka, Osaka 560-8531, Japan*
[2]*Institute for Solid State Physics, University of Tokyo, Kashiwanoha, Kashiwa, Chiba 277-8581, Japan*
(Received 3 September 2008; published 9 October 2008)

We have grown single crystals of a triangular lattice antiferromagnet (TLA), $CuCrO_2$, and investigated the correlation between magnetic and dielectric properties. Two magnetic phase transitions are observed at $T_{N2} \approx 24.2$ K and $T_{N1} \approx 23.6$ K. It was found that ferroelectric polarization along the triangular lattice plane develops at T_{N1}, suggesting that the system undergoes a transition into an out-of-plane 120° spin-chiral phase at T_{N1}. The TLA provides an opportunity for unique magnetoelectric control of spin-chiral ferroelectric domain structures by means of electric and/or magnetic fields.

DOI: 10.1103/PhysRevB.78.140401 PACS number(s): 75.80.+q, 75.30.Kz, 77.80.−e

Spin chirality, i.e., handedness of an ordered magnetic state, in frustrated magnets showing noncollinear spin structure, has been extensively discussed because it has been theoretically predicted to play an important role in magnetic ordering of frustrated systems, such as spin glasses[1,2,4] and spiral magnets.[3,4] However, it is not straightforward to detect and control the chirality which is multispin variable defined by original spin variables. Polarized neutron-diffraction technique has been recently developed as a powerful method to detect the chirality directly.[5] Furthermore, some experimental methods and ideas which can control the chirality were proposed.[6–8] However, these studies have not yet been fully substantiated owing to limitation of experimental facilities and requirement of a large single crystal. Thus, establishing a novel and simpler technique to study the spin chirality is greatly desirable.

Recently, it has been discussed that many frustrated noncollinear spiral magnets show ferroelectricity through a strong magnetoelectric coupling.[9] Most of the magnetically driven ferroelectrics such as $TbMnO_3$ (Ref. 10) exhibit cycloidal-spiral magnetic orders in which the plane of the spiral is parallel to the magnetic modulation vector Q. The microscopic origin of the ferroelectricity is successfully explained by the spin-current mechanism[11] or the inverse Dzyaloshinskii-Moriya (DM) mechanism.[12] In these mechanisms, the direction of ferroelectric polarization is perpendicular to Q and parallel to the spiral plane. In addition, the sign of ferroelectric polarization is determined by that of the vector spin chirality, which has been confirmed by polarized neutron-diffraction measurements.[13] Thus, in frustrated spiral magnets, one can approach the magnetism by electric control of the chirality through the magnetoelectric coupling.

One of the most typical frustrated magnetic structures is a 120° spin structure in a triangular lattice antiferromagnet (TLA), in which three spins form 120° angles with neighboring spins.[4] This spin structure is the most ideal object to investigate the magnetoelectric correlation because of its *simple commensurate* spiral structure. Two types of the 120° spin structures appear on TLA, depending on the sign of single-ion anisotropy D.[14] With $D>0$ (easy-plane type), a 120° structure whose spin spiral plane is parallel to the triangular lattice plane (TLP) emerges (in-plane 120° structure), whereas in the case of $D<0$ (easy-axis type), a 120° structure whose spiral plane is normal to the TLP shows up (out-of-plane 120° structure). Within the framework of the spin-current (or inverse DM) model, macroscopic polarization vanishes in both the in-plane and the out-of-plane 120° structures. However, ferroelectricity in the in-plane 120° structure has been recently reported for $RbFe(MoO_4)_2$, which has been discussed by symmetry-based phenomenological theory.[15]

Our target in the present work is a TLA showing the out-of-plane 120° structure, $CuCrO_2$ with the delafossite structure (space group $R\bar{3}m$) [the inset of Fig. 1(a)]. The magnetic properties are dominated by Cr^{3+} ions ($3d^3$, $S=3/2$) forming TLPs, and are well represented by a $S=3/2$ Heisenberg

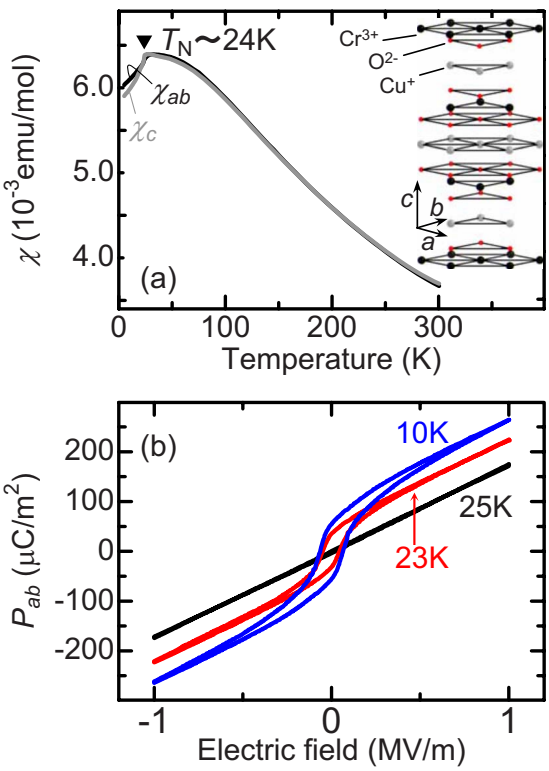

FIG. 1. (Color online) (a) Temperature profiles of χ_c (gray line) and χ_{ab} (black line) for a single crystal of $CuCrO_2$. (b) P_{ab} versus electric field at selected temperatures. Inset of (a): crystal structure of $CuCrO_2$.

 ©2008 The American Physical Society

TLA. A neutron powder diffraction study has reported that $CuCrO_2$ undergoes magnetic ordering into the out-of-plane 120° structure below $T_N \approx 25$ K because of $D<0$.[16] Although, very recently, ferroelectricity below T_N has been reported for $CuCrO_2$, no anisotropic information (e.g., direction of polarization) has been provided for lack of single-crystal measurements.[17] In this paper, we investigated the correlation between magnetic and dielectric properties in single crystals of $CuCrO_2$. We show possible detection and control of the spin chirality through the magnetoelectric coupling.

Single crystals of $CuCrO_2$ were successfully grown from Bi_2O_3 flux. The obtained crystals had a plate shape ($\sim 4 \times 4 \times 0.5$ mm^3) with the widest plane perpendicular to the hexagonal c axis. For the measurement of dielectric constant ε and electric polarization P, they were cut into thin plates with the widest plane parallel and perpendicular to the c axis. Subsequently, silver electrodes were vacuum deposited onto the opposite faces of the crystals. We measured ε at 1 kHz by an *LCR* meter. Temperature profiles of P were obtained by integration of pyroelectric current in the warming process after a poling electric field (400 kV/m) was applied in the cooling process from ~35 to 5 K. Specific heat C and dc magnetic susceptibility χ were measured by using a Quantum Design physical property measurement system (PPMS) by means of a relaxation method and a magnetic property measurement system (MPMS) superconducting quantum interference device (SQUID) magnetometer, respectively.

Figure 1(a) shows temperature dependence of χ parallel to the c axis (χ_c) and ab plane (χ_{ab}). A clear anomaly is observed for the χ_c at $T_N \sim 24$ K due to magnetic phase transition, which is consistent with the previous studies.[16–19] Above 150 K, both χ_c and χ_{ab} data are well described by a Curie-Weiss law. The Weiss temperatures θ estimated as 211 K and 203 K for χ_c and χ_{ab}, respectively, are much larger than T_N. Figure 1(b) shows P parallel to the ab plane (P_{ab}) versus electric field E applied along the ab plane at selected temperatures. P_{ab} shows a linear E dependence without hysteresis above T_N, while clear hysteresis loops were observed at temperatures below T_N. These results ensure that ferroelectricity is induced by the out-of-plane 120° spin structure in $CuCrO_2$, as reported in Ref. 17.

To elucidate more details of the magnetic and ferroelectric transition, we show temperature profiles of χ, C, ε, and P near T_N in Figs. 2(a)–2(d). As seen in Fig. 2(a), χ_c drops at $T_{N2} \approx 24.2$ K while χ_{ab} shows a small but clear anomaly at $T_{N1} \approx 23.6$ K, indicating two successive magnetic phase transitions occur. This is confirmed by temperature profile of C [Fig. 2(b)] showing two peaks almost at T_{N1} and T_{N2}. These two anomalies have reproducibility observed in different specimens. Although a recent specific-heat measurement for a polycrystalline sample has detected only one peak at ~25 K,[19] this discrepancy may be ascribed to accuracy of measurements or sample quality. Previous studies on other Heisenberg TLAs with easy-axis anisotropy ($D<0$) such as $CsNiCl_3$ revealed that there are two successive magnetic phase transitions, where ordering of the spin components parallel and perpendicular to the hexagonal c axis occurs at T_2 and T_1 ($T_2 > T_1$), respectively.[14] This means that a collinear and the out-of-plane 120° spin structure appears in the intermediate phase ($T_1 < T < T_2$) and the low-temperature phase ($T < T_1$), respectively. Accordingly, it is plausible that similar successive transitions (paramagnetic-collinear-out-of-plane 120° spin) occur at T_{N2} and T_{N1} for $CuCrO_2$.

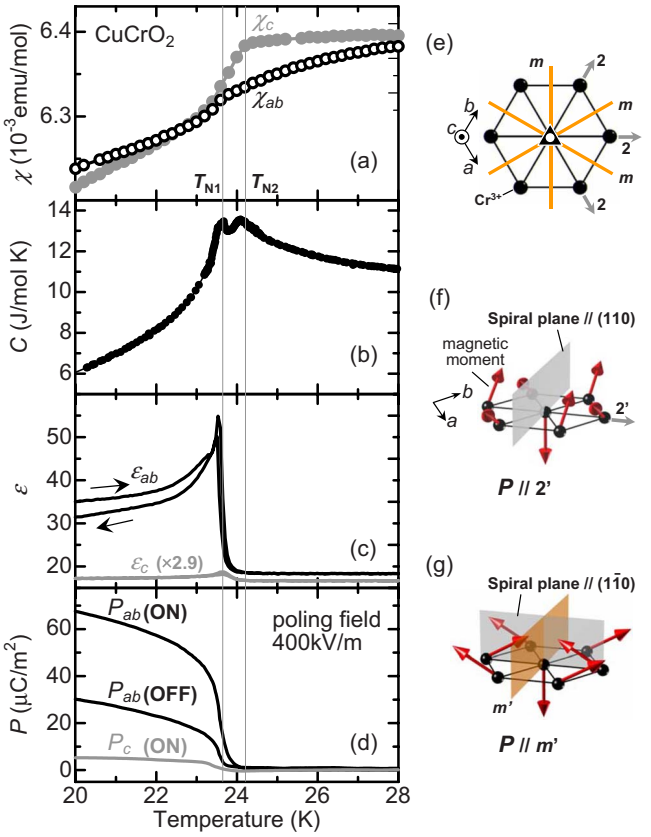

FIG. 2. (Color online) Temperature profiles of (a) χ_c (gray closed circles) and χ_{ab} (black open circles), (b) C, (c) ε_c (gray line) and ε_{ab} (black line) at 1 kHz, and (d) P_c (gray line) and P_{ab} (black line). Measurement of P_c and P_{ab} in (d) were performed with (ON) or without (OFF) electric field of 400 kV/m after poling the crystal. (e) The (001) projection of Cr^{3+} trigonal layer and symmetry operations (2, m, and $\bar{3}$) in $CuCrO_2$. (f), (g) Spin configurations with the remained symmetry operation in the case of the spiral plane parallel to the (110) and the $(1\bar{1}0)$ planes, respectively. Gray (light gray) and orange (dark gray) planes denote the spiral plane and the m' plane, respectively.

As shown in Fig. 2(c), a distinct peak structure is observed at T_{N1} in ε parallel to the ab plane (ε_{ab}) while no substantial structure is seen in that parallel to the c axis (ε_c). Neither ε_{ab} nor ε_c exhibits any anomaly at T_{N2}. Figure 2(d) shows P parallel to the ab plane (P_{ab}) and the c axis (P_c). They were measured with or without applying E of 400 kV/m, labeled "ON" or "OFF," respectively. We observed a symmetric sign reversal of P by applying negative E (−400 kV/m) in the poling process (not shown). Although P_{ab}(OFF) emerges below T_{N1}, P_{ab}(ON) appears at a temperature slightly higher than T_{N1}. This is explained as follows: ferroelectric phase prevails up to higher temperature because it should be more stable in applied E. Thus, temperature profile of P_{ab} indicates that the ferroelectricity is induced by the ordering from the collinear into the 120° spin phase. It should be noticed that P_c(ON) below T_{N1} is by an

order of magnitude smaller than P_{ab}(ON), which may be caused by some misalignment of the samples, representing that the direction of P is within the ab plane.

Here, we discuss the direction of P in the out-of-plane 120° spin structure based on our experimental results and the symmetry analysis. Figure 2(e) depicts the (001) projection of Cr^{3+} trigonal layers with symmetry operations: threefold rotation axis with an inversion center (triangle with small circle), twofold rotation axis (2), and reflection mirror (m). Seki and coworkers[17] pointed out that it is needed to consider two different spin configurations for the out-of-plane 120° spin structure proposed in Ref. 16. One of the configurations is illustrated in Fig. 2(f), where the spin spiral plane is parallel to the (110) plane. In this spin structure, only a $2'$ symmetry operation, twofold rotation around the [110] axis followed by performing time-reversal, remains unbroken. Hence, only spontaneous polarization along the $2'$ direction is allowed, which is consistent with our experimental result. The other configuration possesses the spiral plane parallel to the $(1\bar{1}0)$ plane [Fig. 2(g)]. In this case only an m' symmetry operation, mirror reflection normal to the $[1\bar{1}0]$ axis followed by performing time-reversal, remains unbroken. Accordingly, spontaneous polarization is permitted within the m' plane. However, our experimental observation ($P \| ab$) ensures that P is normal to the spiral plane. In either spiral spin arrangement, the direction of P is normal to the spiral plane. Consequently, these results indicate that the spin configuration with the (110) spiral plane is a more plausible ground-state structure of $CuCrO_2$. We emphasize that the measurement of P on single-crystal samples helps us to determine the spin configuration.

Let us now consider the microscopic mechanism of the ferroelectricity in $CuCrO_2$. The spin-current scenario[11] and the inverse DM scenario[12] cannot explain the ferroelectricity in $CuCrO_2$ as in other TLAs showing spiral magnetic orders without cycloidal component [e.g., $RbFe(MoO_4)_2$ (Ref. 15) and $CuFe_{1-x}Al_xO_2$ (Refs. 20–22)]. Recently, Arima[23] predicted that the proper-screw spiral spin order in a low-symmetry crystal can induce ferroelectricity through a variation in the metal-ligand hybridization with spin-orbit coupling. This scenario well explains the ferroelectricity in $CuFe_{1-x}Al_xO_2$ showing a proper-screw order, and can also be applicable to that in $CuCrO_2$. Arima's mechanism implies that the change in helicity of the screw causes the polarization reversal, which was experimentally confirmed in $CuFe_{1-x}Al_xO_2$.[22] Thus, the ferroelectric property of the TLA $CuCrO_2$ is expected to be used for detection and control of the spin chirality.

We also investigated the effect of magnetic fields ($H \leq 8$ T) on the ferroelectric polarization. Figures 3(a)–3(c) show the temperature profiles of P_{ab}(ON) in H parallel to P_{ab} ($H_{ab} \| P_{ab}$), perpendicular both to P_{ab} and the c axis ($H_{ab} \perp P_{ab}$), and along the c axis ($H_c \perp P_{ab}$), respectively. With the $H_{ab} \| P_{ab}$ configuration P_{ab}(ON) increases with increasing H_{ab} [Fig. 3(a)], while P_{ab}(ON) drastically decreases with increasing H_{ab} in the $H_{ab} \perp P_{ab}$ setup [Fig. 3(b)]. No change of P_{ab}(ON) is observed by applying H_c [Fig. 3(c)]. It is worth mentioning that P_c(ON) is insensitive to the application of H (not shown).

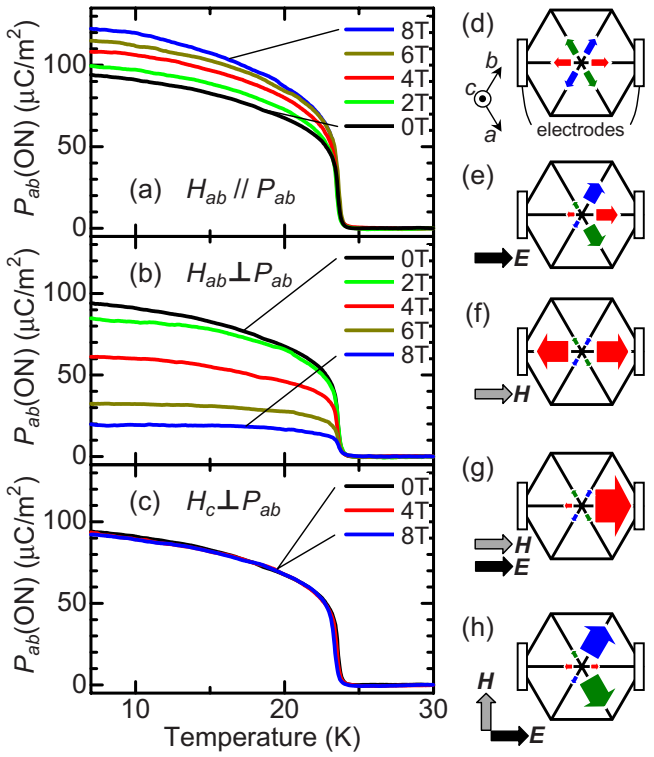

FIG. 3. (Color online) Temperature profiles of P_{ab}(ON) at selected magnetic fields (a) $H_{ab} \| P_{ab}$, (b) $H_{ab} \perp P_{ab}$, and (c) $H_c \perp P_{ab}$ for a single crystal of $CuCrO_2$. (d)–(h) Schematic illustrations of ferroelectric domain configurations in various types of external fields in the situation where the (110) spiral plane is realized and electrodes are deposited onto the (110) plane. Thick arrows denote the directions of P of the respective existing ferroelectric domains. The size of arrows schematically corresponds to the volume of each ferroelectric domain.

To discuss the magnetic-field effects, we need to consider the domain configuration of the out-of-plane 120° spin structure. Given a sixfold symmetry in the triangular lattice plane, the 120° spin structure is triply degenerated, that is, three spiral-plane domains exist, which are at 120° angle with each other. Taking also into account of the doubly degenerated spin chirality, a total of six magnetic domains should exist without any external fields. Considering the one-to-one relation between the signs of P and the spin chirality, as well as between the direction of P and the spiral plane above mentioned, there exist six spin-chiral ferroelectric domains, (i.e., 60°-domain structures). In the following discussion, for simplicity, we consider only the situation where the (110) spiral plane is realized and electrodes are deposited onto the (110) plane. Note that even with the $(1\bar{1}0)$ spiral plane and other setup of electrodes, the conclusion of the discussion remains unchanged.

Figures 3(d)–3(h) show schematic drawings of spin-chiral ferroelectric domains with or without external fields during poling process. In the absence of both E and H, six domains coexist equivalently [Fig. 3(d)]. Since these six domains are degenerated, each domain has the same volume as the others. Hence net polarization P_{ab} becomes zero. When a poling *electric* field is applied, finite P_{ab} can be detected because

domains with polarization component parallel (not "antiparallel") to E become stable [Fig. 3(e)].

Next, we discuss the effects of H on these domains. Using the magnetic susceptibility perpendicular ($\chi_\perp$) and parallel ($\chi_\parallel$) to the spiral plane, we can express χ_c and χ_{ab} as $\chi_c = \chi_\parallel$ and $\chi_{ab} = (\chi_\parallel + \chi_\perp)/2$. (These equations are obtained from simple geometric calculations.) Since χ_{ab} is slightly larger than χ_c below T_{N1} [see Figs. 1(a) and 2(a)], $\chi_\perp > \chi_\parallel$ is obtained. Accordingly, when only H along [110] is applied, the domains with the spiral plane parallel to the (110) plane is stabilized, that is, the ferroelectric domains with P along $\pm H$ becomes stable [Fig. 3(f)]. Such a rearrangement of spiral-plane domain by applying H has been reported for $CsNiBr_3$ showing the out-of-plane 120° spin structure,[24] supporting our prediction for $CuCrO_2$.

Supposing this prediction, we can simply understand the magnetic-field effects on P_{ab}(ON). By applying $H_{ab} \| P_{ab(\|[110])}$, the ferroelectric domains should shift from Fig. 3(e) to Fig. 3(g), well explaining the increase in P_{ab}(ON) as displayed in Fig. 3(a). By applying $H_{ab} \| P_{ab(\|[110])}$, the ferroelectric domains switch from Fig. 3(e) to Fig. 3(h) because the domain with P along [110] becomes unstable. Since this domain gives the largest contribution to P_{ab}(ON), the decrease in P_{ab}(ON) by applying $H_{ab} \perp P_{ab}$ can be well described. Thus, our results strongly suggest that the domains of the chirality and the spiral plane can be controlled by electric and magnetic fields, respectively.

In summary, we investigated magnetic and dielectric properties of $CuCrO_2$ single crystals. We found that $CuCrO_2$ undergoes two successive magnetic phase transitions, probably into a collinear antiferromagnetic structure and then the out-of-plane 120° spin structure. Ferroelectricity appears in the out-of-plane 120° spin phase where the spin chirality develops, indicating the spin chirality can be detected and controlled through magnetoelectric coupling. Triangular lattice antiferromagnets showing the out-of-plane 120° spin structure provide an opportunity for a unique control of spin-chiral ferroelectric domain structures by using electric and/or magnetic fields.

We thank Y. Sekio, M. Hagiwara, and H. Kawamura for fruitful discussions. This work was supported by KAKENHI (Contracts No. 20674005 and No. 20001004) and the 21st Century COE Program (Project No. G18) of the JSPS.

[1] J. Villain, J. Phys. C **10**, 4793 (1977).
[2] S. Miyashita and H. Shiba, J. Phys. Soc. Jpn. **53**, 1145 (1984).
[3] M. L. Plumer and A. Mailhot, Phys. Rev. B **50**, 16113(R) (1994).
[4] H. Kawamura, J. Phys.: Condens. Matter **10**, 4707 (1998); Can. J. Phys. **79**, 1447 (2001), and references therein.
[5] V. P. Plakhty, J. Kulda, D. Visser, E. V. Moskvin, and J. Wosnitza, Phys. Rev. Lett. **85**, 3942 (2000).
[6] K. Siratori, J. Akimitsu, E. Kita, and M. Nishi, J. Phys. Soc. Jpn. **48**, 1111 (1980).
[7] M. L. Plumer, H. Kawamura, and A. Caillé, Phys. Rev. B **43**, 13786(R) (1991).
[8] V. I. Fedorov, A. G. Gukasov, V. Kozlov, S. V. Maleyev, V. P. Plakhty, and I. A. Zobkalo, Appl. Phys. A: Mater. Sci. Process. **224**, 372 (1997).
[9] T. Kimura, Annu. Rev. Mater. Res. **37**, 387 (2007), and references therein.
[10] M. Kenzelmann, A. B. Harris, S. Jonas, C. Broholm, J. Schefer, S. B. Kim, C. L. Zhang, S.-W. Cheong, O. P. Vajk, and J. W. Lynn, Phys. Rev. Lett. **95**, 087206 (2005).
[11] H. Katsura, N. Nagaosa, and A. V. Balatsky, Phys. Rev. Lett. **95**, 057205 (2005).
[12] I. A. Sergienko and E. Dagotto, Phys. Rev. B **73**, 094434 (2006).
[13] Y. Yamasaki, H. Sagayama, T. Goto, M. Matsuura, K. Hirota, T. Arima, and Y. Tokura, Phys. Rev. Lett. **98**, 147204 (2007).
[14] M. F. Collins and O. A. Petrenko, Can. J. Phys. **75**, 605 (1997), and references therein.
[15] M. Kenzelmann, G. Lawes, A. B. Harris, G. Gasparovic, C. Broholm, A. P. Ramirez, G. A. Jorge, M. Jaime, S. Park, Q. Huang, A. Ya. Shapiro, and L. A. Demianets, Phys. Rev. Lett. **98**, 267205 (2007).
[16] H. Kadowaki, H. Kikuchi, and Y. Ajiro, J. Phys.: Condens. Matter **2**, 4485 (1990).
[17] S. Seki, Y. Onose, and Y. Tokura, Phys. Rev. Lett. **101**, 067204 (2008).
[18] J. P. Doumerc, A. Wichainchai, A. Ammar, M. Pouchard, and P. Hagenmuller, Mater. Res. Bull. **21**, 745 (1986).
[19] T. Okuda, Y. Beppu, Y. Fujii, T. Onoe, N. Terada, and S. Miyasaka, Phys. Rev. B **77**, 134423 (2008).
[20] T. Kimura, J. C. Lashley, and A. P. Ramirez, Phys. Rev. B **73**, 220401(R) (2006).
[21] S. Seki, Y. Yamasaki, Y. Shiomi, S. Iguchi, Y. Onose, and Y. Tokura, Phys. Rev. B **75**, 100403(R) (2007).
[22] T. Nakajima, S. Mitsuda, S. Kanetsuki, K. Tanaka, K. Fujii, N. Terada, M. Soda, M. Matsuura, and K. Hirota, Phys. Rev. B **77**, 052401 (2008).
[23] T. Arima, J. Phys. Soc. Jpn. **76**, 073702 (2007).
[24] M. Sano, K. Iio, and K. Nagata, Phys. Rev. B **39**, 9753(R) (1989).